

# Optical characterization of gold-cuprous oxide interfaces for terahertz emission applications

Gopika K. P. Ramanandan,<sup>1,\*</sup> Aurèle J. L. Adam,<sup>1</sup> Gopakumar Ramakrishnan,<sup>1</sup> Peter Petrik,<sup>1,2</sup> Ruud Hendrikx,<sup>3</sup> and Paul C. M. Planken<sup>1</sup>

<sup>1</sup>*Optics Research Group, Faculty of Applied Physics, Delft University of Technology, Lorentzweg 1, 2628 CJ Delft, The Netherlands*

<sup>2</sup>*Research Institute for Technical Physics and Materials Science, H-1525 Budapest, P.O. Box 49, Hungary*

<sup>3</sup>*Department of Materials Science and Engineering, Delft University of Technology, Mekelweg 2, 2628 CD Delft, The Netherlands*

## Abstract

We show that the interface between gold and thermally-formed cuprous oxide, which emits terahertz radiation when illuminated with ultrafast femtosecond lasers is, in fact, an AuCu/Cu<sub>2</sub>O interface, due to the formation of the thermal diffusion alloy AuCu. The alloy enables the formation of a Schottky-barrier-like electric field near the interface which is essential to explain the THz emission from these samples. We confirm the formation of this AuCu layer by X-ray diffraction measurements, ellipsometry and visual inspection. We determined the frequency-dependent complex refractive indices of the Cu<sub>2</sub>O and AuCu layer, and verified them using reflection spectroscopy measurements. These refractive indices can be used for optimizing the thickness of Cu<sub>2</sub>O for maximum THz emission from these interfaces.

*OCIS codes:* 310.6860, 300.6495, 310.6870, 120.2130

---

\* Corresponding author: g.r.kottayipilappara@tudelft.nl

## 1. Introduction

Many metal/semiconductor interfaces emit THz radiation when excited with femtosecond laser pulses [1, 2]. The laser pulses optically generate charge carriers in the semiconductor and the THz emission is the result of carrier acceleration by the electric depletion field that can naturally form near a metal/semiconductor interface. In general, the THz emission is weak when the metal is deposited on top of the semiconductor. This poor THz generation efficiency results from the power loss of the pump laser pulses and of the generated THz pulses in the metal film, and from the fact that light is also absorbed in a region of the semiconductor where there is no depletion field. Recently, we showed that the THz emission of inverted structures, ultra-thin semiconductor layers deposited on gold, is much stronger [3]. When an optimum thickness of the semiconductor layer is chosen, multiple reflections occur inside the layer, which acts as an anti-reflection coating, increasing the absorption within the semiconducting thin film. This effect, also known as cavity-enhanced optical absorption [4], ensures that the maximum absorption occurs in the Schottky-depletion layer, where it matters for the THz generation. One of the surprising results of this work is that cuprous oxide ( $\text{Cu}_2\text{O}$ ) thin films deposited on gold substrates emit strong THz pulses in this manner. The emission is particularly unexpected because the interfaces formed by depositing Au on  $\text{Cu}_2\text{O}$  are ohmic junctions, rather than Schottky junctions [5].

Here, we show optical (and X-ray) measurements of the interface layer between Au and  $\text{Cu}_2\text{O}$  which demonstrate that oxidation of Cu on Au leads to the formation of a CuAu *alloy* and to the formation of a Schottky-like barrier between the alloy and the  $\text{Cu}_2\text{O}$ . We have determined the frequency-dependent complex refractive indices of this alloy and also of the thin  $\text{Cu}_2\text{O}$  film, using variable-angle spectroscopic ellipsometry. The reflection spectra, calculated with these refractive index values, agree well with the measurements. The optical data is particularly interesting and useful for the optimization of the optical absorption and THz emission from these interfaces.

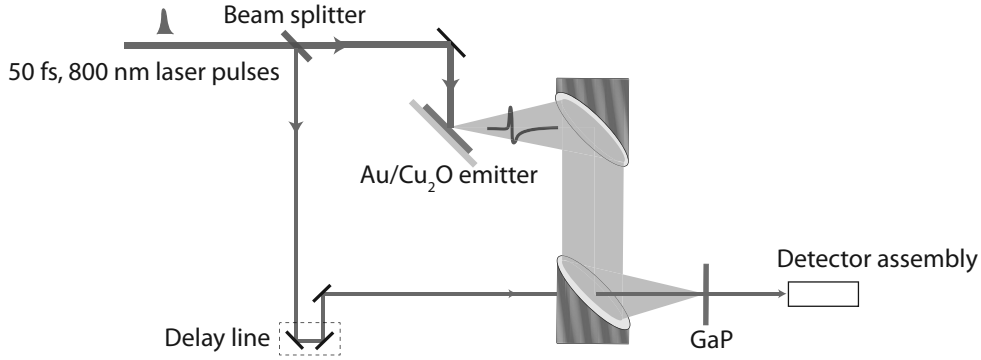


Fig. 1: THz generation set-up: Ultrafast laser pulses are incident on  $\sim 400$  nm thick  $\text{Cu}_2\text{O}$  film deposited on a Au substrate, at  $45^\circ$  angle of incidence. Parabolic mirrors are used to collect, collimate and focus the emitted THz pulses onto a GaP electro-optic crystal. A probe laser beam is also focussed onto the GaP crystal. The detector assembly measures the instantaneous THz electric field in the GaP detection crystal as a change in the polarization state of the probe laser beam.

## 2. Terahertz generation

### 2.A. Sample preparation

Gold substrates are prepared by electron-beam evaporation of Au onto a clean silicon wafer in vacuum. A thin film of chromium is also evaporated onto the silicon substrate prior to the deposition of gold, in order to improve the adhesion of gold to the silicon substrate. The chromium and gold layers are each 50 nm thick. A thin film of copper is then evaporated onto the gold substrate. The Cu thin film is then completely oxidized by thermal oxidation in ambient air at a temperature of  $220^\circ\text{C}$ , to get  $\text{Cu}_2\text{O}$  thin films. The thickness of the  $\text{Cu}_2\text{O}$  thin film formed after oxidation is about 1.5 times that of the original copper thin film. Although copper can form at least two types of stable oxides, it has been observed that for temperatures lower than  $250^\circ\text{C}$ ,  $\text{Cu}_2\text{O}$  is predominantly formed [6, 7].

The experimental set-up used for our THz generation measurements is schematically shown in Fig. 1. We use 50 fs laser pulses from a Ti:Sapphire laser centered at a wavelength of 800 nm. The average power of the laser source is 2.5 W and the repetition rate is 5.2 MHz. The laser beam is split into pump and probe beams by a 90:10 beam splitter. 90% of the laser power is used for the generation of THz pulses from the Au/ $\text{Cu}_2\text{O}$  thin films. The samples

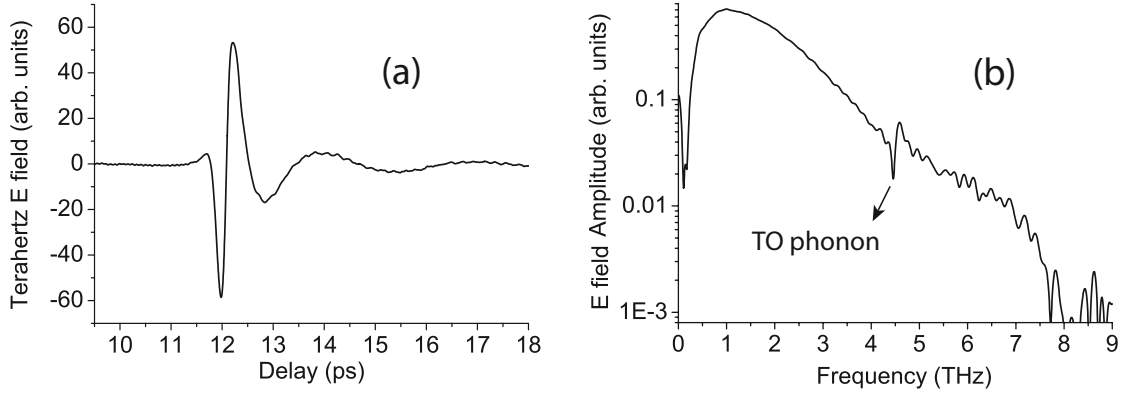


Fig. 2: (a) Time-dependent electric field of the THz pulse emitted from the Au-Cu<sub>2</sub>O Schottky junction and (b) the corresponding Fourier-transformed spectrum.

are mounted in a reflection-type configuration, and the laser is incident on the sample at an angle of 45°. The pump pulses are delayed using a retro-reflecting mirror arrangement mounted on a translation stage. The generated THz pulses are collected, collimated and focussed onto a 300  $\mu\text{m}$  GaP crystal which acts as an electro-optic detection crystal [8]. The probe beam is also focussed onto the detection crystal through an aperture in the last parabolic mirror. The electric field of the THz pulse modifies the polarization state of the 800 nm probe beam which is measured using an arrangement of a quarter wave plate, a Wollaston prism, and a differential detector. The setup is purged with dry nitrogen gas in order to reduce the absorption by water vapor in the atmosphere. The spectrum of the measured THz pulse is obtained by Fourier-transforming the time-dependent THz electric field.

The electric field emitted by a 420 nm thick Cu<sub>2</sub>O thin film on gold and the corresponding Fourier-transformed spectrum are shown in Fig. 2. The bandwidth of the emitted THz pulse ranges from 0.1 to almost 7.5 THz. Interestingly, the TO phonon resonance of Cu<sub>2</sub>O at  $\sim 4.5$  THz [9] can be seen in the THz emission spectrum, indicating that the Cu<sub>2</sub>O thin film is polycrystalline in nature.

### 3. Interfacial alloy formation

The most plausible explanation for THz generation from Au/Cu<sub>2</sub>O junctions is carrier acceleration by the Schottky barrier electric field near the Au/Cu<sub>2</sub>O interface. However, earlier

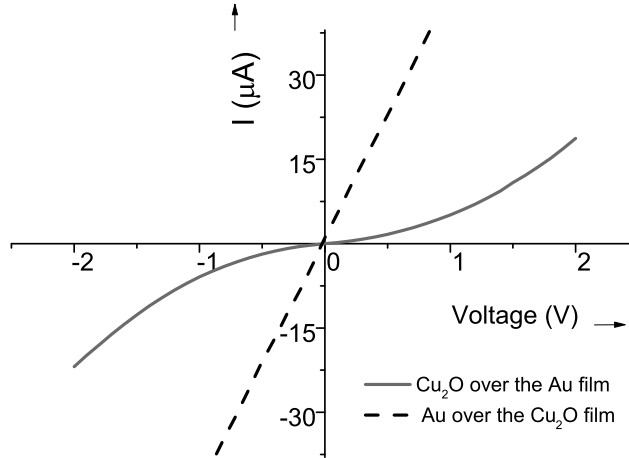


Fig. 3: Measured current-voltage (I-V) characteristics of the Au/Cu<sub>2</sub>O junctions. The solid line shows the junction characteristics of a Cu<sub>2</sub>O thin film fabricated over a Au thin film substrate and the dashed line shows the same when the Au thin film is deposited over the Cu<sub>2</sub>O thin film. The difference in the junction characteristics between the two cases is explained on the basis of diffusion of Cu into the gold film to form an AuCu alloy in the first case, when the oxide layer is thermally formed on the Au film.

reports indicate that the junctions formed when Au is deposited on Cu<sub>2</sub>O, are essentially ohmic in nature [5]. In order to verify the Schottky junction formation when Cu<sub>2</sub>O thin films are fabricated on gold substrates, we measured the current voltage (I-V) characteristics of one of the samples. The measured I-V characteristic of such a sample is shown by the solid red line in Fig. 3. We can see that the junction formed by the oxidation of a Cu film deposited on Au has a non-linear I-V curve. We also made a sample where, first, the Cu was deposited and oxidized to Cu<sub>2</sub>O, followed by the deposition of Au. The junction formed by this sample is characterized by a linear I-V curve (dashed line in Fig. 3), typical of an ohmic junction. This interesting result can be explained as follows. The barrier height of a Schottky interface depends on the work function of the metal. The samples used for terahertz emission experiments are thermally formed Cu<sub>2</sub>O thin films on gold substrates. During the process of heating copper to get the oxide film, inter-metallic compounds or alloys of Au/Cu can be formed by diffusion [10]. In our experiments, this would mean that the interface we have is not an Au-Cu<sub>2</sub>O interface, but an AuCu-Cu<sub>2</sub>O interface. This can cause the junction characteristics to differ from the one with a pure Au/Cu<sub>2</sub>O interface. Note that although the non-linearity of the I-V curve is indicative of a barrier formation, a deviation

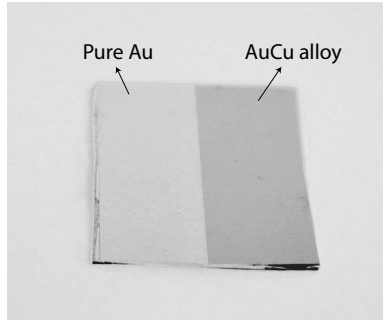


Fig. 4: A photograph of the AuCu alloyed sample surface. The right side of the sample was alloyed, and has a slightly different, rose-gold, color. The left side of the sample is a pure gold surface. The image was processed to obtain a better color contrast.

from the ideal behavior of a Schottky diode is observed. The nearly point symmetric nature of the observed I-V curve is currently under investigation.

In order to investigate the presence of such a diffusion layer, we removed the thermal oxide film from the gold substrate by treating it with dilute nitric acid. A color contrast-enhanced photograph of a pure gold substrate and a gold substrate after removing the  $\text{Cu}_2\text{O}$  film is shown in Fig. 4. The surface of the gold substrate, obtained after removal of the oxide layer, has a rose-gold color, clearly indicating the presence of an interfacial diffusion layer [11]. To confirm this, X-ray analysis of these substrates was also performed.

X-ray diffraction patterns were recorded in a Bragg-Brentano geometry in a Bruker D5005 diffractometer equipped with a Huber incident-beam monochromator and Braun PSD detector. Data collection was carried out at room temperature using Cu  $\text{K}\alpha_1$  radiation as the source. Evaluation of the measured data was done with the Bruker program EVA. All patterns are background-subtracted, meaning that the contribution of air scatter and possible x-ray fluorescence radiation, is subtracted.

The XRD pattern obtained from the cleaned gold substrate with the rose-gold surface is shown in Fig. 5 in black. The colored sticks correspond to the peak positions and intensities of Au and of the AuCu alloy, taken from the ICDD pdf4 database [12]. The intensity vs  $2\theta$  values from the ICDD database correspond to the diffraction pattern from powdered samples with no preferential crystal orientation. It is possible to confirm the presence of a material if the position of the measured diffraction peaks in the  $2\theta$  axis matches with the position of the peaks in the database (the colored sticks). We see that in our measurement,

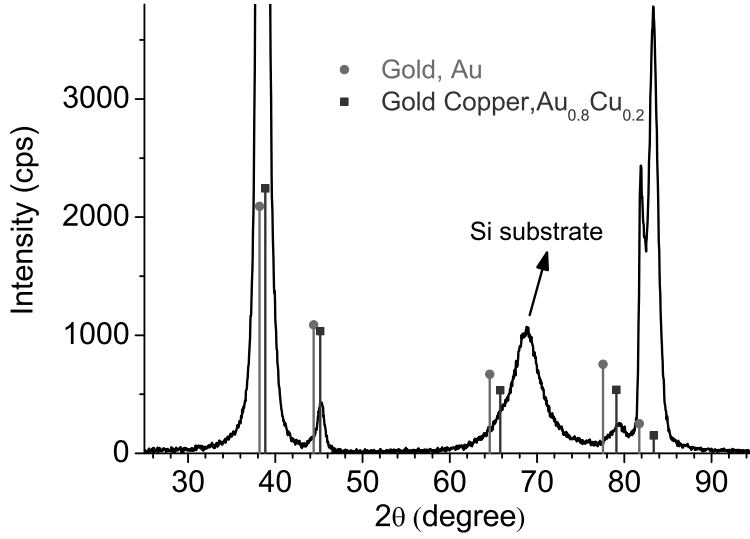


Fig. 5: XRD measurement of the gold substrates from which oxide was removed. No trace of oxide was found in the substrate.

the measured diffraction peak positions coincide with the peak positions of a Au-Cu alloy, in addition to gold and the silicon substrate. The electron-beam evaporated thin metal films usually have a preferred *crystallographic* orientation and, hence, the ratio between the intensities of diffraction peaks don't correspond to that of the *powdered* sample given in the database. The measured x-ray diffraction peak at a  $2\theta$  value of  $39^\circ$  suggests the presence of both Au and AuCu in the sample, but around angles  $45^\circ$ ,  $79^\circ$  and  $83^\circ$ , the measured peaks coincide better with the expected peak positions of the AuCu alloy. This proves that inter-diffusion compounds of Au and Cu are formed at the interface. From the peaks around  $38^\circ$  and  $82^\circ$ , it can be argued that some Au is also present in its pure form. From the XRD analysis, the alloy is estimated to have a composition of  $\text{Au}_{0.8}\text{Cu}_{0.2}$ . However, since nitric acid can dissolve Cu, we note that the process of removing the  $\text{Cu}_2\text{O}$  layer could have caused some changes in the actual composition of the alloy layer. Moreover, the composition of the alloy may vary in depth and laterally due to inhomogeneities in the diffusion. The main intention here is to show the presence of an inter-diffusion layer, and its importance in the THz generation process from our samples.

#### 4. Variable Angle Spectroscopic Ellipsometry (VASE) measurements

Spectroscopic ellipsometry allows for accurate measurements of the optical properties of thin films. In this technique, the change in polarization state of the light reflected from the thin film-substrate system is measured and is expressed by two values ( $\Psi$ ,  $\Delta$ ) which are defined by the ellipsometric equation [13, 14]

$$e^{i\Delta} \tan(\Psi) = \rho = \frac{r_p}{r_s}. \quad (1)$$

Here  $r_p$  and  $r_s$  are the complex Fresnel reflection coefficients of the sample for p and s polarized incident light.  $\Psi$  and  $\Delta$  represent the angles determined from the amplitude ratio and phase difference between the reflected p- and s-polarized components, respectively. A model is constructed to calculate the values of ( $\Psi$ ,  $\Delta$ ) using various parameters such as optical constants, layer thickness, surface roughness, etc. The generated and the experimentally determined values of  $\Psi$  and  $\Delta$  are compared and one or more model parameters are adjusted to fit the experimental data. This is done in an iterative manner until a good fit is reached between the measured and the experimental spectra. In variable angle spectroscopic ellipsometry, these values are measured over a wide range of wavelengths and angles of incidence, which helps to minimize errors in extracting the material properties.

We performed ellipsometric measurements using a Variable Angle Spectroscopic Ellipsometer (VASE, J.A.WoollamCo.) in the wavelength region from 600 nm to 1600 nm and at different angles of incidence varying from 45° to 60°. Initially, we fabricated individual thin films of Au and Cu<sub>2</sub>O on silicon wafers, and measured the ( $\Psi$ ,  $\Delta$ ) values of the light reflected from these samples. The refractive indices were obtained from the best fit model. The gold film was modelled to have a Drude-like conductivity. The frequency-dependent refractive indices of the gold film were measured because the properties of a thin film deposited by e-beam evaporation may be different from that of the bulk, since they depend on the conditions of evaporation like the chamber pressure, rate of deposition, etc.

We then measured the ( $\Psi$ ,  $\Delta$ ) values of the light reflected from a thin Cu<sub>2</sub>O film on Au, formed by the thermal oxidation of copper. Based on the assumption that there is an inter-diffusion layer of AuCu formed at the interface, we included this layer in the model. Hence, the model consists of the AuCu alloy film on gold (which was considered as the substrate), and the Cu<sub>2</sub>O layer with surface roughness. At the start of the fitting procedure, the thickness of the pure gold film and the AuCu alloy was set to 50 nm and 0 nm, respectively,



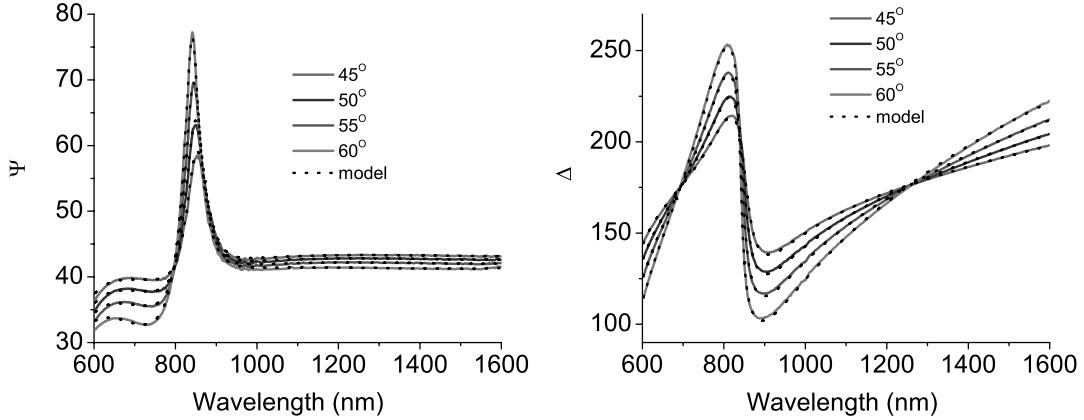


Fig. 6:  $\Psi$  and  $\Delta$  measurements of the light reflected from a  $\text{Cu}_2\text{O}$  thin film on gold substrate (lines). The dots show the values of  $\Psi$  and  $\Delta$  calculated from the model used.

Both  $\Psi$  and  $\Delta$  are plotted in units of degrees.

and was then allowed to vary during the iterations. The refractive index of AuCu was allowed to vary in the model, and the frequency-dependent refractive indices of the material were parameterized by means of B-splines, which provide a numerical tool for data fitting, without considering any physical model [15]. A B-spline consists of an array of control or 'knot' points and a set of interpolating polynomial functions. The permittivity values of the material assumed by the model at the knot points are so as to generate  $(\Psi, \Delta)$  values, which match with the experimentally measured ones. The imaginary part of the frequency-dependent dielectric permittivity of the material is modeled as the B-spline function and the real part is calculated from the Kramers-Kronig relations. The imaginary part of the refractive index,  $k$  is forced to be always positive, to make physical sense. Measured optical constants of the evaporated 50 nm Au film were used as the starting values for fitting that of the AuCu film. The frequency-dependent refractive indices of the  $\text{Cu}_2\text{O}$  thin film were also parameterized by means of B-splines. For  $\text{Cu}_2\text{O}$ , the initial values of the refractive index were taken from the measured values for a different oxide film on a silicon substrate.

The values of  $\Psi$  and  $\Delta$  for the sample from the experiment and the best-fit model are shown in Fig. 6. The colored solid lines correspond to the measured  $\Psi$  and  $\Delta$  at different angles of incidence and the dashed black lines show the values calculated using the model. A good fit is obtained between the measurement and the model, as can be seen from the figure. The optical constants of the Au-Cu alloy and  $\text{Cu}_2\text{O}$  from the best-fit model are given in Fig. 7. The thickness of the  $\text{Cu}_2\text{O}$  thin film was around 232 nm with a roughness of

23 nm. This agrees well with the average roughness ( $\sim 21$  nm) measured using the AFM. Increasing the thickness did not have any effect on the model-generated values of  $(\Psi, \Delta)$ , indicating that the thickness of the AuCu film is larger than the penetration depth. The penetration depth of light of wavelength 700 nm in the AuCu thin film was calculated to be around 8 nm.

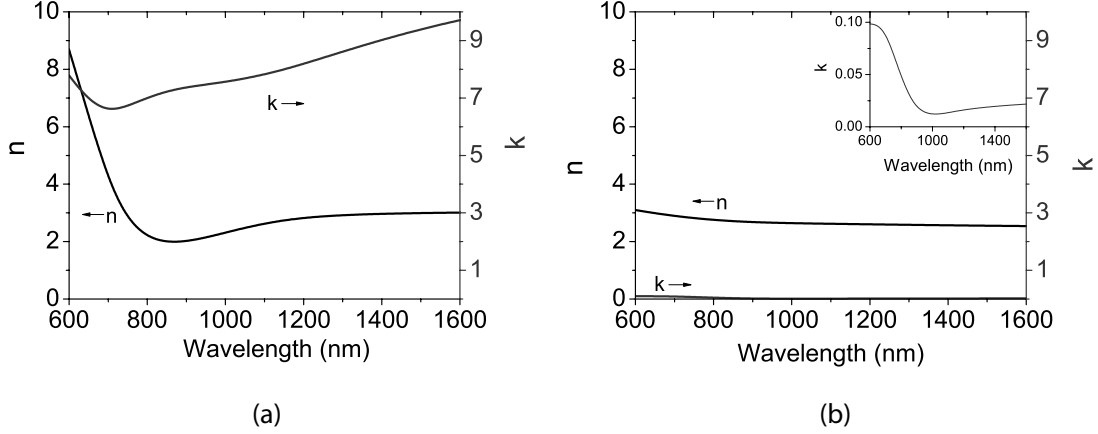


Fig. 7: Frequency dependent real ( $n$ ) and imaginary ( $k$ ) parts of the refractive index of (a) the AuCu interdiffusion layer, and (b) the  $\text{Cu}_2\text{O}$  thin film, as obtained using the VASE software. The inset of (b) gives a closer look at the imaginary part of the refractive index of the  $\text{Cu}_2\text{O}$  thin film.

## 5. Multilayer reflection: Calculation and experiment

The THz emission from a  $\text{Cu}_2\text{O}/\text{Au}$  interface is proportional to the amount of laser power absorbed in the oxide film. At an optimum thickness, the  $\text{Cu}_2\text{O}$  film can act as its own antireflection coating and hence increase the absorption inside the sample at a particular wavelength. Knowing the reflection spectra of the  $\text{Cu}_2\text{O}$  thin films on oxide substrates we can find the thickness at which the reflection minimum occurs at the pump laser wavelength, 800 nm. Since we have extracted the frequency-dependent refractive indices of the  $\text{Cu}_2\text{O}$  and AuCu thin films, we can calculate the reflection spectra of the oxide films on the AuCu substrate for various thicknesses. We also experimentally measured the broadband reflection spectra of samples of five different  $\text{Cu}_2\text{O}$  thicknesses on AuCu substrates, to validate the complex refractive indices of the materials obtained from the ellipsometer analysis.

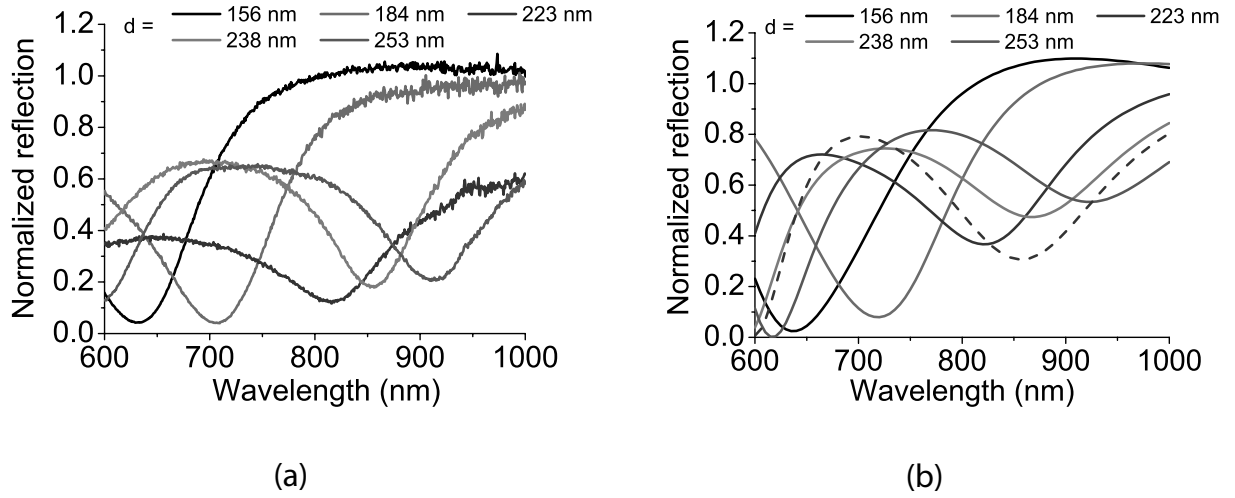


Fig. 8: White light reflection spectra from  $\text{Cu}_2\text{O}$  layers of different thicknesses 'd' on an AuCu substrate, normalized to the reflection from bare gold substrates. (a) Experimentally measured, (b) calculated from the analytical model using the complex refractive indices of the materials obtained from the ellipsometry analysis. The dashed blue line shows the calculated reflection spectrum of a  $\text{Cu}_2\text{O}$  thin film of thickness 223 nm on pure Au.

To measure the reflection spectrum, a Tungsten halogen lamp (HL 2000, Ocean optics) was used as the broadband visible light source. The light from the source was passed through a polarizer and was incident upon the samples at  $45^\circ$  angle of incidence. The spectrum of the reflected light was measured using an Ocean Optics spectrometer. The  $\text{Cu}_2\text{O}$  layer thicknesses of the samples used in the experiment were estimated using the variable angle spectroscopic ellipsometer. The intensity of the light reflected from the oxide film on the gold substrate was measured as a function of wavelength and normalized to the reflection from a bare gold film. The reflectivity spectra thus obtained for five different  $\text{Cu}_2\text{O}$  film thicknesses are plotted in Fig. 8(a). The calculation of the wavelength-dependent reflectivity, also normalized to the reflection from a bare gold film, was done with an analytical solution [16] which is suitable for multilayers containing strong absorbing elements such as metals. The calculated reflection spectra are shown in Fig. 8(b). The multilayer stack considered for the reflection coefficient calculation consists of the silicon substrate, a 50 nm thick Cr film, 50 nm AuCu layer and the  $\text{Cu}_2\text{O}$  film. To calculate the reflection spectra, we used the frequency-dependent complex refractive index of the materials, obtained from analyzing the ellipsometry measurements. We can see that there is a good agreement between the

calculated and the measured reflection spectra. The dashed blue curve in Fig. 8(b) shows the calculated reflection spectrum of a sample with a 223 nm thick  $\text{Cu}_2\text{O}$  film on a pure Au substrate, rather than on a AuCu alloy substrate. It can be seen that this does not match well with the experimentally measured spectrum for the same oxide thickness. In particular, the position of the calculated minimum at  $\sim 855$  nm is off compared to the measured one at  $\sim 820$  nm. A good agreement between the measured and calculated reflection spectra is obtained only when the AuCu thin film was considered in the calculation, again supporting the presence of the inter-diffusion AuCu alloy layer and validating the optical constants derived from the ellipsometer measurements. The thickness of the oxide layer of this sample was also measured independently using a surface profilometer to be  $\sim 225$  nm. The slight discrepancies between the calculated and measured reflection spectra could be due to a combination of several issues. The reflection calculation, for example, ignores the roughness of the oxide film in the calculation, the lateral inhomogeneities in the refractive index of the  $\text{Cu}_2\text{O}$  layer, and experimental errors in determining the angle of incidence. It can also be seen from the calculated and reflected spectra that an oxide film of  $\sim 223$  nm thickness is well suited for THz emission applications, since it has a very low reflection coefficient at 800 nm, which is the pump laser wavelength used in THz generation experiments.

## 6. Conclusions

We have shown that interfaces between gold and thermal  $\text{Cu}_2\text{O}$ , which emit THz radiation when illuminated with ultrafast femtosecond lasers, are in fact AuCu/ $\text{Cu}_2\text{O}$  interfaces, due to the formation of thermal diffusion induced alloy of AuCu at the interface. This alloy plays an important role in the THz emission by enabling the formation of a Schottky-barrier-like junction. The presence of the alloy layer has been confirmed using X-ray diffraction measurements, ellipsometry and visual inspection. The optical properties of the alloy and  $\text{Cu}_2\text{O}$  thin films have been characterized using variable angle spectroscopic ellipsometry, and were used to calculate the reflection spectra which agree well with the measurements.

## 7. Acknowledgements

P. C. M. P. and A. J. L. A. acknowledge the financial support from the Nederlandse Organisatie voor Wetenschappelijk Onderzoek (NWO) and the Stichting voor Technische Wetenschappen (STW) in the form of VICI and VENI grants respectively.

## References

- [1] X. Zhang, J. T. Darrow, B. B. Hu, D. H. Auston, M. T. Schmidt, P. Tham, and E. S. Yang, “Optically induced electromagnetic radiation from semiconductor surfaces,” *Appl. Phys. Lett.* **56**, 2228–2230 (1990).
- [2] Y. Jin, X. F. Ma, G. A. Wagoner, M. Alexander, and X. C. Zhang, “Anomalous optically generated THz beams from metal/GaAs interfaces,” *Appl. Phys. Lett.* **65**, 682–684 (1994).
- [3] G. Ramakrishnan, G. K. P. Ramanandan, A. J. L. Adam, M. Xu, N. Kumar, R. W. A. Hendrikx, and P. C. M. Planken, “Enhanced terahertz emission by coherent optical absorption in ultrathin semiconductor films on metals,” *Opt. Express* **21**, 16784–16798 (2013).
- [4] W. Wan, Y. Chong, L. Ge, H. Noh, A. D. Stone and H. Cao, “Time-reversed lasing and interferometric control of absorption,” *Science* **331**, 889–892 (2011).
- [5] L. C. Olsen, R. C. Bohara, and M. W. Urie, “Explanation for low-efficiency  $\text{Cu}_2\text{O}$  Schottky-barrier solar cells,” *Appl. Phys. Lett.* **34**, 47–49 (1979).
- [6] G. Papadimitropoulos, N. Vourdas, V. E. Vamvakas, and D. Davazoglou, “Deposition and characterization of copper oxide thin films,” *J. Phys: Conf. Ser* **10**, 182 (2005).
- [7] G. K. P. Ramanandan, G. Ramakrishnan, and P. C. M. Planken, “Oxidation kinetics of nanoscale copper films studied by terahertz transmission spectroscopy,” *J. Appl. Phys.* **111**, 123517-6 (2012).
- [8] N. C. J. van der Valk, T. Wenckebach, and P. C. M. Planken, “Full mathematical description of electro-optic detection in optically isotropic crystals,” *J. Opt. Soc. Am. B* **21**, 622-631 (2004).
- [9] Y. P. Yang, W. C. Wang, Z. W. Zhang, L. L. Zhang, and C. L. Zhang, “Dielectric and lattice vibrational spectra of  $\text{Cu}_2\text{O}$  hollow spheres in the range of 1-10 THz,” *J. Phys. Chem. C* **115**, 10333–10337 (2011).

- [10] R. Morrish, K. Dorame, and A. Muscat, “Formation of nanoporous Au by dealloying AuCu thin films in HNO<sub>3</sub>,” *Scripta Mater.* **64**, 856 – 859 (2011).
- [11] C. Cretu and E. van der Lingen, “Coloured gold alloys,” *Gold Bulletin* **32**, 115–126 (1999).
- [12] J. Faber and T. Fawcett, “The powder diffraction file: present and future,” *Acta Crystall. B* **58**, 325–332 (2002).
- [13] J. A. Woollam, B. D. Johs, C. M. Herzinger, J. N. Hilfiker, R. A. Synowicki, and C. L. Bungay, “Overview of variable-angle spectroscopic ellipsometry (VASE): I. Basic theory and typical applications,” in “Society of Photo-Optical Instrumentation Engineers (SPIE) Conference Series,” (1999), pp. 3–28.
- [14] H. Fujiwara, *Spectroscopic Ellipsometry: Principles and Applications* (Wiley, New York, 2007).
- [15] J. W. Weber, T. A. R. Hansen, M. C. M. Van de Sanden, and R. Engeln, “B-spline parametrization of the dielectric function applied to spectroscopic ellipsometry on amorphous carbon,” *J. Appl. Phys.* **106**, 123503–9 (2009).
- [16] O. El Gawhary, M. C. Dheur, S. F. Pereira, and J. J. M. Braat, “Extension of the classical Fabry-Perot formula to 1D multilayered structures,” *Appl. Phys. B* **111**, 637–645 (2013).